A Novel Rod−Coil Block Copolymer and Its Compatible Blends

Jin Wu, Eli M. Pearce,* and T. K. Kwei

Department of Chemical Engineering and Chemistry, Herman F. Mark Polymer Research Institute, Polytechnic University, 6 MetroTech Center, Brooklyn, New York 11201

Received June 30, 2000; Revised Manuscript Received December 4, 2000

ABSTRACT: A novel rod−coil diblock copolymer, poly(*n*-hexyl isocyanate)-*b*-poly(ethylene glycol) (PHIC-*b*-PEG) was synthesized by using the living titanium(IV)-catalyzed coordination polymerization method. The lyotropic mesophases and mesophases in solid state of the PHIC-*b*-PEG rod−coil block copolymer were investigated using polarized optical microscopy (POM). The 30 wt % copolymer/toluene solution exhibited birefringence with apparent orientation. The morphology in the solid state showed nematic-like domain structures. The sizes of the domains decreased when the solid film was solution-cast from chloroform rather than toluene. However, the overall dimension of the domain was estimated to be micrometer in scale. The solution-cast PHIC-*b*-PEG/PMMA blends showed some compatibility between the two components from the DSC measurements. The 5/95 (wt/wt) blend exhibited liquid crystalline domains of 1-μm size. The 40/60 blend indicated improved compatibility. The tensile strength of the more compatible 40/60 blend was significantly improved especially at high temperatures around T_g. The creep experiments at various temperatures above T_g showed reorientation of the rods in the 40/60 blend. These ordered domains in the blend were further confirmed by DSC, where a small sharp endothermic peak appeared at around 140 °C with an enthalpy change about 0.4 J/g. This melting of the stretch-induced ordering of the rods was irreversible.

Introduction

Rod−coil block copolymers, which consist of a rigid rod block and a flexible coil block, have attracted much research interest because of both the science and potential applications behind this novel class of self-assembling polymers. To date, a number of experimental studies of synthetic rod−coil macromolecules have been reported with regard to their phase behavior, self-assembly and microstructures.[1] Theoretical studies have already predicted major differences between rod−coil block copolymers and coil−coil block copolymers a few years earlier.[2] However, much more research needs to be explored to clearly understand the connection between theoretical predictions and experimental results.

Recently, a number of new mesomorphic rigid-rod polymers have been synthesized which has generated interest in forming composites by blending them with conventional flexible-coil polymers.[3,4] Compared to miscible blends that are well mixed at the molecular level, these blends are called compatible with domain sizes around micrometer. Potential improvements in fracture, impact toughness, and dimensional stability have been targeted for finding a method for dispersing rigid molecules finely and uniformly in the matrix. However, the strong tendency for self-aggregation of rigid molecules must be overcome. In addition, the adhesion at the interface between the rigid molecule and the matrix must be strong enough to withstand the shear stress generated at the interface when the force is applied. To improve the interfacial adhesion, one possible way is to blend rod−coil block copolymers or hairy-rod polymers (more like rod−coil graft copolymers) with the matrix instead of rigid-rod polymers themselves. The "coil" component in rod−coil block copolymer or the "hair" component in hairy-rod polymer is able to mix well with the matrix polymer, thereby improving the interfacial adhesion.

To date a number of rod−coil block copolymers[1] and hairy-rod polymers[5] have been synthesized and characterized. However, the studies of blending these copolymers with homopolymers were very few. Takayanagi[3] reported molecular composites of aramid block copolymers with aliphatic nylons, which were statistically isotropic. Recently, Zin et al.[6] studied the solubilization behavior of poly(ethylene oxide) (PEO) into a rod−coil block copolymer of ethyl 4-[4′-oxy-4-biphenylcarbonyloxy]-4′-biphenycarboxylate-*b*-PEO (BCEO-12), in which PEOs were partially miscible with the PEO block of the copolymer.

In this paper, a novel rod−coil diblock copolymer, poly(*n*-hexyl isocyanate)-*b*-poly(ethylene glycol) (PHIC-*b*-PEG), was synthesized and characterized. PHIC was reported to adopt a 12_5 helical structure[7] and appear as a stiff rod in a wide range of solvents such as toluene and chloroform.[8,9a] The inherent chain stiffness of PHIC is primarily due to short-range restrictions to rotation, and it has a persistence length of about 50−60 nm.[9b] The designed copolymer consisted of a hydrophobic rigid-rod PHIC block and a hydrophilic flexible-coil PEG block. In this investigation, blends of the copolymer PHIC-*b*-PEG with a homopolymer including poly(methyl methacrylate) (PMMA) or poly(vinyl acetate) (PVAc) were studied using thermal analysis and optical microscopy techniques. Martuscelli et al.[10] studied the phase structure in PEO/PMMA blends, and they found the blends were compatible but the interactions were very weak. They also found PEO/PVAc blends[11] were compatible through relatively weak favorable intermolecular interactions. Shih et al.[12] demonstrated the tacticity effects on the miscible behavior of PMMA/poly(ethylene oxide)-*b*-poly(dimethylsiloxane)-*b*-poly(ethylene oxide) blends. Thus, in PHIC-*b*-PEG/PMMA blends or PHIC-*b*-PEG/PVAc blends, the PEG block is expected to be compatible with the homopolymer.

The mesophases including lyotropic mesophases and solid state mesophases of rod−coil block copolymers are a relatively unexplored research area. Liquid crystalline ordering was observed in concentrated solutions (>15

10.1021/ma0011486 CCC: $20.00
Published on Web 02/06/2001

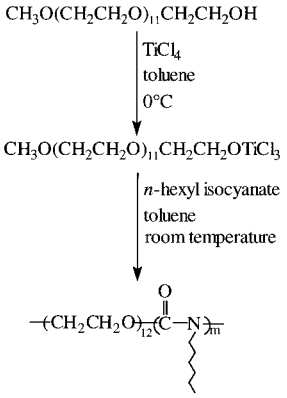

Figure 1. Synthetic scheme for the preparation of the PHIC-*b*-PEG rod−coil block copolymer.

wt %) of the polystyrene-*b*-poly(*n*-hexyl isocyanate) rod−coil block copolymer, and a new zigzag morphology was revealed in the solid state.[1b] In addition, morphologies consisting of fragmented PS zigzags and micellelike regions were observed. Lee et al. reported that a rod−coil copolymer (BCEO-12) had a monolayer lamellar structure with alternating rod- and coil-rich domains.[1g] At room temperature, the BCEO-12 molecule was crystalline and transformed into a smectic A phase at an elevated temperature. In this investigation, the mesophases of the PHIC-*b*-PEG rod−coil block copolymer were studied. By converting the rod configuration of the PHIC block into the coil configuration induced by pentafluorophenol (PFP)[13] as cosolvent in solution, we compared the morphologies of solution-cast films from both the rod−coil block copolymer and the coil−coil block copolymer.

Experimental Section

Materials. Poly(ethylene glycol) methyl ether (M_n = 550, M_w/M_n = 1.08) was supplied by Aldrich Chemical Co., Inc. Titanium(IV) chloride (1.0 M solution in toluene) and *n*-hexyl isocyanate (97%) were purchased from Aldrich. Poly(vinyl acetate) (MW = 60 000) was obtained from Polysciences, Inc., and poly(methyl methacrylate) (MW = 30 000) and pentafluorophenol (99%+) were purchased from Aldrich. All other chemical and reagents were of chemical grade.

Synthesis of Poly(*n*-hexyl isocyanate)-*b*-poly(ethylene glycol) (PHIC-*b*-PEG). The PHIC-*b*-PEG rod−coil diblock copolymer was synthesized using the living titanium(IV)-catalyzed coordination polymerization method, which was developed by Novak et al.[14] The synthetic scheme is shown in Figure 1. All syntheses and polymerizations were performed under argon atmosphere. Toluene (solvent) was distilled from Na/benzophenone. The *n*-hexyl isocyanate monomer was distilled from CaH_2 and stored under an argon atmosphere.

The titanium initiator $TiCl_3PEG\text{-}OCH_3$ was synthesized as follows: One milliliter of $TiCl_4$/toulene (1.0 mmol) was added to a 25-mL flask, and cooled to 0 °C using an ice-salt bath. Vacuum-dried poly(ethylene glycol) methyl ether (M_n = 550, 1.0 mmol) was dissolved in 5 mL of dry toluene, and the solution was slowly added to the flask. After 1 h, the ice−salt bath was removed and the reaction flask was purged with rapid flow of argon in order to remove the HCl gas. The reaction was stirred overnight, after which the reaction vessel was evacuated. The solid was redissolved in 5 mL of toluene, and a dark-orange solution was obtained.

The PHIC-*b*-PEG block copolymer was polymerized as follows: To the above dark-orange solution was added *n*-hexyl isocyanate (60 mmol) via a syringe. The polymerization solution turned bright orange immediately. The mixture was stirred for 1 h at room temperature, and was then quenched with chilled methanol. The viscous solution was precipitated in methanol. After several cycles of dissolving and precipitation, a white solid copolymer was obtained and vacuum-dried at room temperature for 4 days.

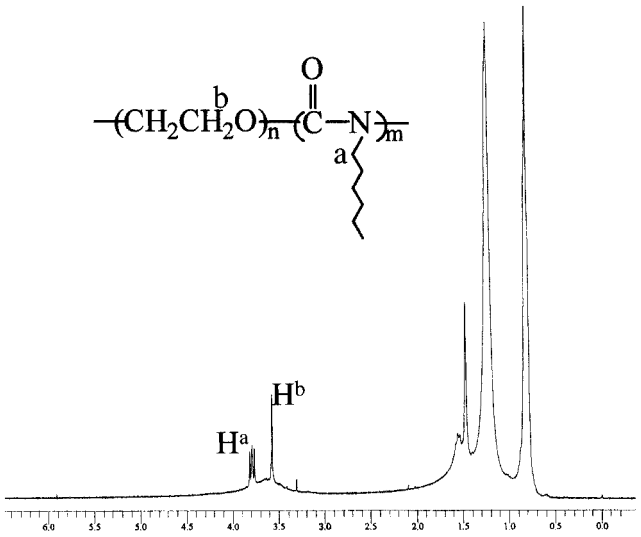

Figure 2. ^1H NMR spectrum of poly(*n*-hexyl isocyanate)-*b*-poly(ethylene glycol).

Characterization of PHIC-*b*-PEG. The product was characterized by ^1H NMR, ^{13}C NMR, GPC, TGA, and (modulated) DSC without further purification. The ^1H and ^{13}C NMR spectra ($CDCl_3$ as solvent) were determined using a Bruker-200 MHz spectrometer. Gel permeation chromatography (GPC) was performed with $CHCl_3$ as the mobile phase. The thermogravimetric analysis (TGA) was carried out on a Hi-Res 2950 TGA from TA instruments with a 10 °C/min heating rate under nitrogen purge. A TA 2920 modulated DSC was operated in both standard and modulated modes. In the standard mode, a heating rate of 10 °C/min was used and the T_g was identified from the inflection point of the specific heat jump. In the modulated mode, a heating rate of 3 °C/min with oscillation amplitude of 0.68 °C and a period of 80 s was adopted. The T_g was identified from the derivative of the heat capacity signal (dC_p/dT).

Preparation of the PHIC-*b*-PEG/PMMA Blends. The solutions (3% w/v) of PHIC-*b*-PEG and PMMA were prepared by dissolving the individual polymer in toluene. Blends of various compositions, which were represented in weight ratios, were made by mixing appropriate amounts of these solutions. Films for subsequent experiments were obtained by casting the solution on glass slides followed by slow evaporation of the solvent at room temperature, and vacuum-drying at 90 °C for 7 days to ensure the complete removal of the residual solvent in the samples. The PHIC-*b*-PEG/PVAc blends were prepared in a similar way.

Dynamic Mechanical Analysis (DMA). The PHIC-*b*-PEG/PMMA (40/60) films were subject to dynamic mechanical analysis with a TA DMA 2980 dynamic mechanical analyzer. A Poisson ratio of 0.44 was chosen for each film sample. The sample geometry was rectangular with a length of ∼15 mm, a width of ∼5 mm, and a thickness of ∼0.2 mm.

The DMA multifrequency experiments were performed under the tension-film mode with the following parameters: a frequency of 1.0 Hz, an oscillatory amplitude of 5.0 μm, a static force of 0.010 N and an auto-tension of 102%. The temperature was ramped from room temperature to 150 °C at a heating rate of 2 °C/min. The storage modulus and the loss modulus were recorded as a function of temperature. For comparison, the PMMA film was prepared and subjected to the same DMA measurement.

The DMA creep experiments were performed at 80, 90, 95, and 100 °C also under the tension-film mode with the following parameters: a displacement of 1.00 MPa and a static force of 0.010 N. The PHIC-*b*-PEG/PMMA (40/60) sample was equilibrated at the designated temperature for 20 min before the

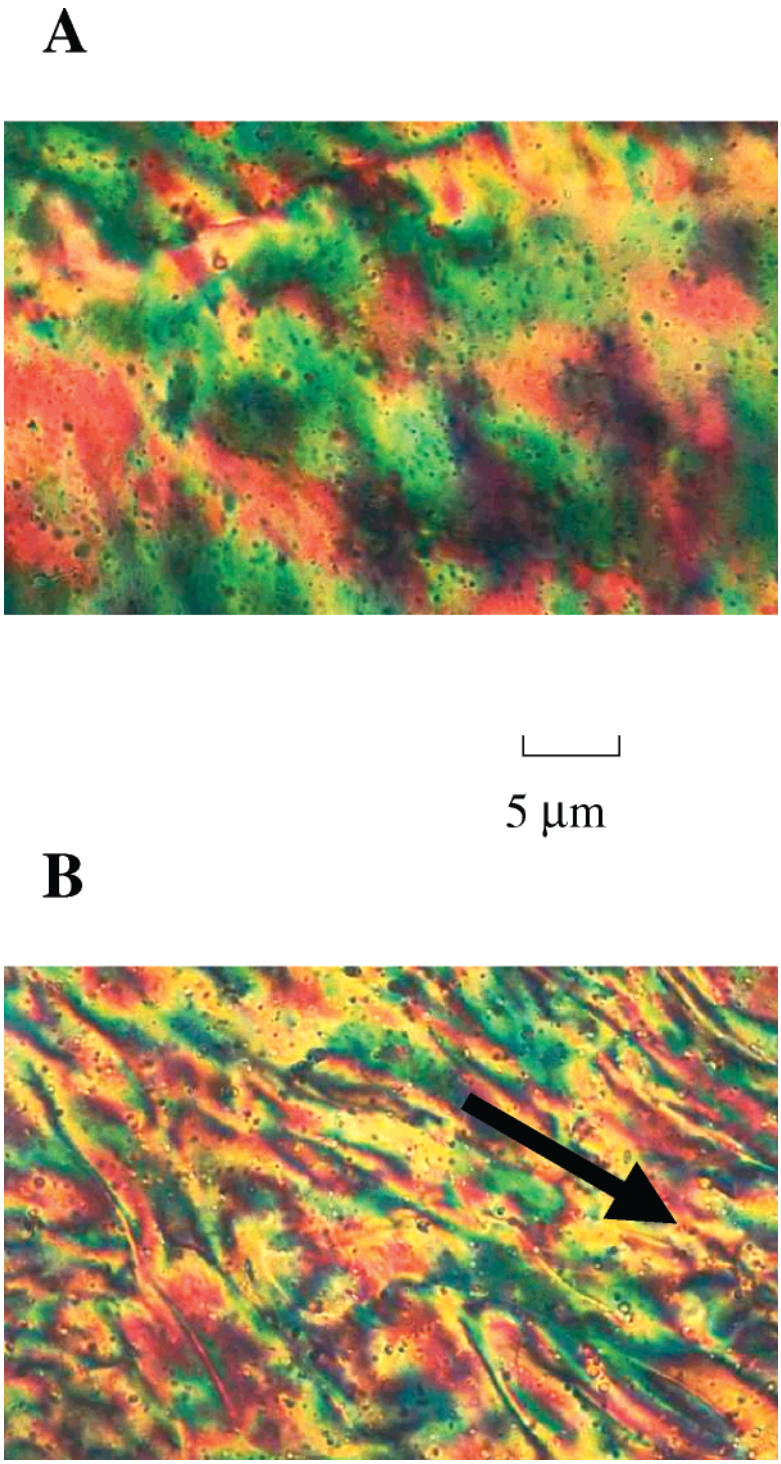

Figure 3. Polarized optical micrographs of (A) 20 and (B) 30 wt % solutions (arrow indicating the apparent orientation direction) of the PHIC-*b*-PEG block copolymer in toluene at room temperature.

creep mode was activated. Immediately after the creep experiment, the film samples were subjected to the DSC measurements.

Differential Scanning Calorimetry (DSC). A TA 2920 DSC unit was used in this study with a heating rate of 10 °C/min. Before DSC measurement, each sample was subject to the TGA measurement using a TA Hi-Res 2950 TGA unit.

Polarized Optical Microscopy (POM). The optical microscope (Nikon Optiphot) equipped with a hot stage (Mettler FP-82) and a Nikon FX-35A camera was used to observe the morphologies of the polymer blends, which were mounted on glass slides by solution casting. The lyotropic mesophase of the PHIC-*b*-PEG block copolymer in concentrated solution was observed under POM using a self-made liquid cell. The morphologies of the copolymer in solid state were observed from solution-casting films on glass slides from different solvents.

Results and Discussion

Synthesis and Characterization of the PHIC-*b*-PEG Rod−Coil Diblock Copolymer. Recently, Patten and Novak[14a] reported the living polymerization of alkyl isocyanates catalyzed by $TiCl_3OCH_2CF_3$. They also explored the effect of modifying the ligand sphere of the end group and the initiating ligand upon polymerization. They found that isocyanate monomers with functional side chains could be polymerized using these

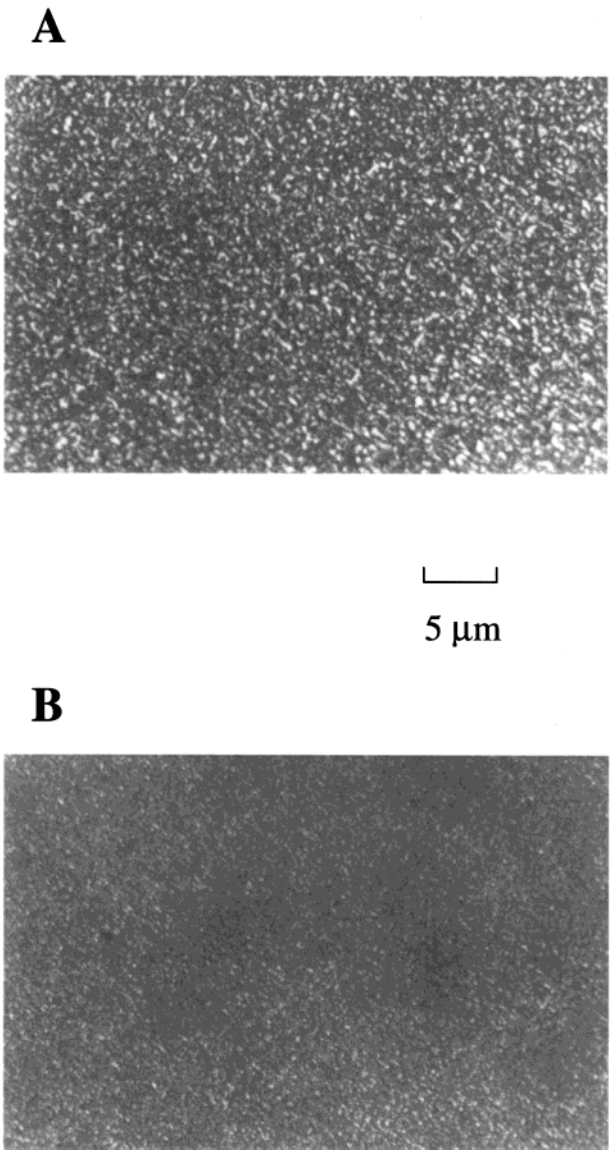

Figure 4. Polarized optical micrographs of the PHIC-*b*-PEG block copolymer derived from the 0.4 wt % (A) toluene and (B) chloroform solutions.

modified initiators. The initiators were of the form of $CpTiCl_2X$, where X = −OR, $-NR_2$, or $-CR_3$ ($C_p = \eta^5$-cyclopentadienyl), C_p*$TiCl_2OR$ (C_p* = η^5-pentamethylcyclopentadienyl), and $C_{p2}TiClOR$.[14b] Polymerizations using C_pTiCl_2X were found to tolerate a wide variety of Lewis bases.

Titanium−alkoxide, −amide, and −alkyl bonds were identified to be active in initiating the insertion of isocyanate monomer.[15] The use of derivatives synthesized from $TiCl_4$ or C_pTiCl_3 provided a general route through which a wide variety of end groups might be incorporated onto the initiating end of the polyisocyanate chain.

Jha[16] reported the synthesis of a water-soluble polyisocyanate, poly(3-(2-(2-methoxyethoxy)ethoxy)propyl isocyanate) (PDEGIC) using $C_pTiCl_2OCH_2CF_3$ as the initiator. Incorporation of the oligo(ethylene glycol) side chain to the isocyanate monomer did not inhibit the polymerization when a titanium(IV) catalyst was used as the initiator.

Accordingly, a novel titanium(IV) catalyst, poly(ethylene glycol)$TiCl_3$ [CH_3O $(CH_2CH_2O)_nTiCl_3$], was designed and used to initiate polymerization of the *n*-hexyl isocyanate monomer. The activities of the initiators are found to depend on the degree of polymerization (*n*) of PEG.

A series of commercially available poly(ethylene glycol) methyl ethers were tested including M_n = 350, 550, 750, 2000, and 5000. The catalyst loses its ability to initiate polymerization when the value of *n* is greater than 17 (M_n = 750), which is partially due to low solubility of PEG in toluene, especially at low temperatures, since the initiator is prepared at ∼0 °C. The C_pTiCl_2PEG type of initiator is not used based on the knowledge that steric bulk may be increased too much at the metal center when a PEG chain is present at the same site.

A series of the rod−coil block copolymers were synthesized, where the degree of polymerization of the PEG block (*n*) was constant at 12 (M_n = 550), but the degree of polymerization of the PHIC block (*m*) was changeable depending on the polymerization conditions. In one case, the *m* value of the block copolymer used is determined to be around 50 (M_n = 6500) by proton NMR. The ^{1}H NMR spectrum is shown in Figure 2, where the triplet peaks at δ = 3.82, 3.79, 3.77 are assigned to the methylene protons directly attaching to the N atom of *n*-hexyl isocyanate; the other triplet peaks at δ = 3.59, 3.58, 3.57 are assigned to the methylene protons of the PEG block. The chemical structure of this PHIC-*b*-PEG block copolymer is also confirmed by ^{13}C NMR (δ = 14.1, 23.0, 26.5, 28.6, 31.9, 58.8, 70.3, 156.7). The polydispersity index of this specific block copolymer is determined to be 1.2 by GPC. This $PHIC_{50}$-*b*-PEG_{12} rod−coil block copolymer was used in the following studies.

The onset degradation temperature of this block copolymer is determined to be 162 °C by TGA. The glass transition of each block was determined by both conventional DSC and temperature-modulated DSC. From the conventional DSC, the T_g of the PEG block is determined to be −67.6 °C, while that of the PHIC block is not detected. With the help of the temperature-modulated DSC, the T_g of the PHIC block is estimated to be at around 10 °C.

Mesophases of the PHIC-*b*-PEG Rod−Coil Block Copolymer. Lyotropic mesophases of coil−coil block copolymers have been investigated in several cases such as polystyrene-*b*-polyisoprene and polystyrene-*b*-poly(ethylene oxide).[17] Both copolymers exhibited the characteristic texture of a hexagonal structure in solution. Lyotropic mesophases of rod−coil block copolymers were studied in this investigation. Lyotropic mesophase of the rod−coil block copolymer in toluene was observed when the concentration exceeded 20 wt %. The polarized optical micrograph of a concentrated solution of the copolymer in toluene (20 wt %), which was viewed at 300x under crossed polarizers, is shown in Figure 3A. The micrograph indicates that the block copolymer solution is birefringent at this concentration. However, the birefringent pattern is not uniform primarily due to the random orientation of the liquid crystalline regions. In contrast, Figure 3B shows an optical micrograph of a 30 wt % solution. The apparent banded texture, which is not very uniform, shows signs of orientation. This characteristic texture was previously observed in sheared solutions of PHIC[18] and PHIC-*b*-PS[1b] and also in drawn PHIC samples.[7] In this study, concentrated solution of the rod−coil block copolymer clearly shows orientation of the liquid crystalline regions

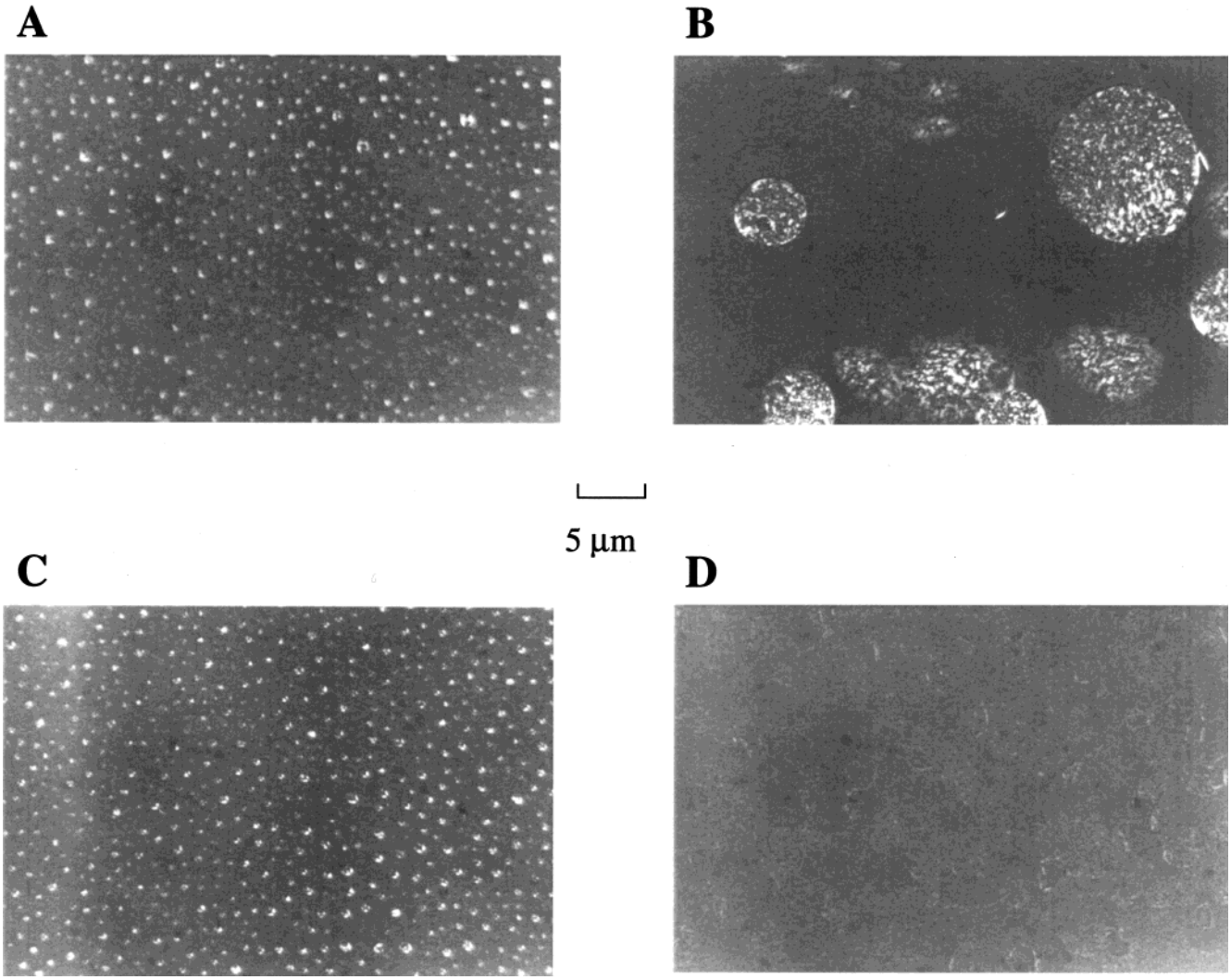

Figure 5. Polarized optical micrographs of (A) the PHIC-*b*-PEG/PMMA blend (5/95), (B) the PHIC-*b*-PEG/PS blend (5/95), (C) the PHIC-*b*-PEG/PVAc blend (5/95), and (D) the PHIC-*b*-PEG/PMMA blend (40/60).

without any shear process. The orientation is induced by the increase in concentration. The POM observations indicate that the PHIC-*b*-PEG rod−coil block copolymer behaves mesogenically on the micrometer scale in length. In addition, when the concentration was further increased above 45 wt %, a transparent gel formed.

The solution-cast copolymer films were prepared from the 0.4 wt % toluene solutions. As can be seen in Figure 4A, the nematic-like domain structures are present in the solid state with domains of ~1 μm in size. The use of different casting solvents such as chloroform and THF does not change the overall texture of the copolymer in the solid state, except that the texture is finer (Figure 4B). The domain sizes are estimated to be less than 1 μm. It is known that chloroform actively interacts with PHIC and slightly alters its conformation. The diameter of the PHIC helical rod is smaller in chloroform than in toluene. This provides a reasonable explanation that the texture of the copolymer is also finer in the chloroform-cast film. Alternatively, the change in texture can be achieved by intentionally converting the helical configuration of the PHIC block to the coil configuration. In this study, we added an excess amount of pentafluorophenol (PFP) to the 0.4 wt % PHIC-*b*-PEG/toluene (mole ratio of PFP to the monomer HIC of 70) to ensure complete conversion of the helices to coils. The solution-cast film was then examined under POM, and no apparent liquid crystalline structures are observed at the same magnification. The POM studies indicate that the behavior of the PHIC-*b*-PEG rod−coil block copolymer is very different from that of the PHIC-*b*-PEG coil−coil block copolymer.

Compatible PHIC-*b*-PEG/PMMA Blends. Blends were prepared as described above at 40/60 and 5/95 weight ratios. In the 5/95 blend, the weight ratio of the two compatible components, PEG and PMMA, is around 0.4/100. However, the miscibility effect already makes a big difference in blend morphology shown in Figure 5A. As can be seen, the copolymer domains (bright spots) with almost uniform dimensions of 1 μm are regularly distributed in the PMMA matrix (dark background). Also, visible macroscopic maltese crosses are present within the copolymer domains, which is caused by a radial symmetrical orientation of the copolymer molecules in the film plane. The optical behavior of the film is correlated with the orientation of the macromolecules, in which black areas between crossed polarizers are the result of macromolecules orientated with their optical axes parallel to the axes of the polarizers. These experimental phenomena of macroscopic structures in liquid crystal systems were also studied and reviewed in the literature.[19−21] These features are in complete contrast with those of a completely immiscible PHIC-

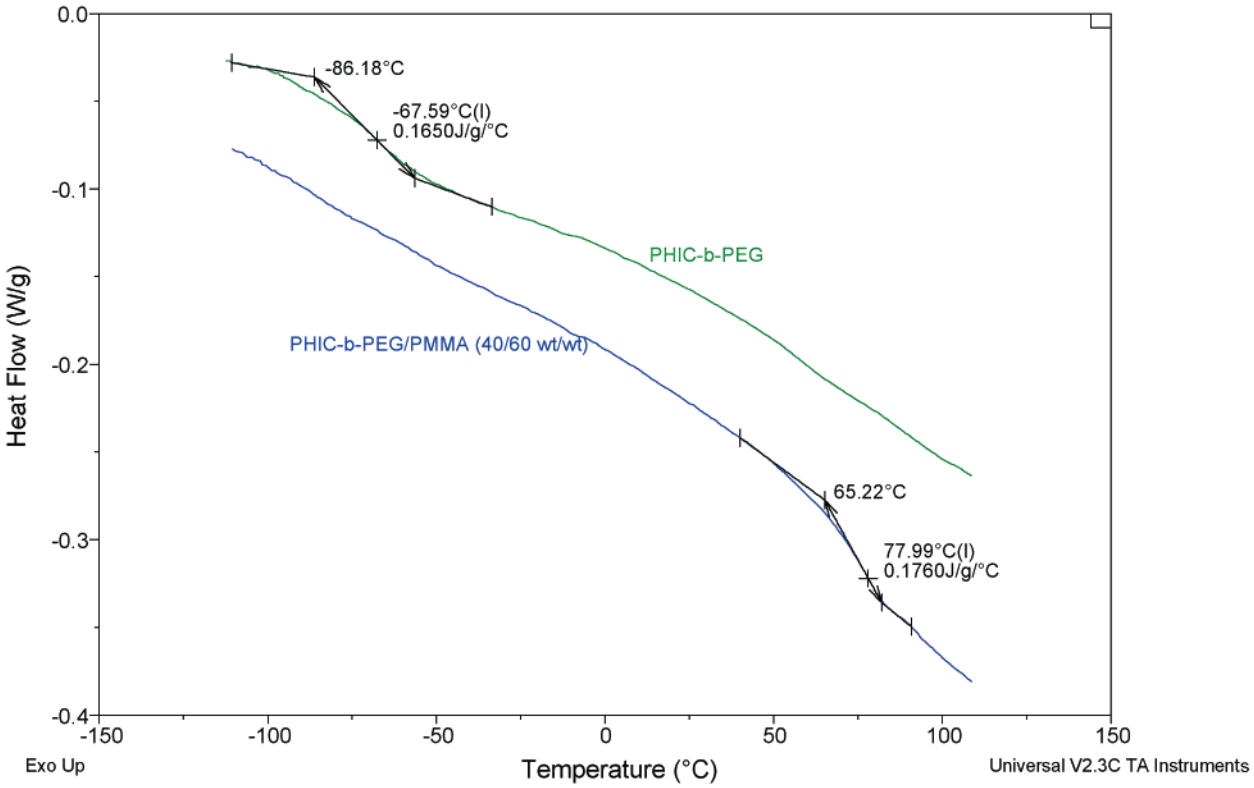

Figure 6. DSC thermograms of the PHIC-*b*-PEG block copolymer and its blend with PMMA (40/60). (The curves were extracted from the second heating run.)

b-PEG/PS (5/95) blend film, which shows gross phase separation with nonuniform copolymer domains of tens of micrometers in scale (Figure 5B).

A similar morphology was observed in the PHIC-*b*-PEG/PVAc blend (5/95), where the PEG block is also expected to be miscible with the poly(vinyl acetate) matrix. The polarized optical micrograph is shown in Figure 5C, where bright copolymer domains of 1 μm in dimension with macroscopic maltese crosses are present in the dark PVAc matrix. As in the case of PMMA matrix, the tiny amount of the PEG block attached to the rigid-rod PHIC polymer suffices to reduce drastically the domain size. Therefore, it is a very promising way to disperse a rigid-rod polymer in a polymer matrix by using a rod−coil block copolymer, in which the coil block is miscible with the matrix. The ultimate goal to molecularly dispersing a rigid-rod polymer in a polymer matrix is not achieved, which we expect highly depends on the relative weight ratio of the two blocks as well as the strength of the compatibility between the coil block and the polymer matrix.

The PHIC-*b*-PEG/PMMA blend was further investigated by using a higher content of the copolymer component. The 40/60 blend films prepared from solution casting to have a thickness around 200 μm were used for DSC and DMA measurements. The DSC curve presented in Figure 6 is from the second heating run after the first heating−cooling cycle. The heating and cooling rates were controlled at 10 °C/min. The DSC curve for the rod−coil block copolymer is also shown for comparison. As seen from the copolymer curve, the glass transition temperature of the PEG block is detected at around −68 °C (inflection point), and that of the PHIC block is not detected. The PEG block shows no melting endotherm, most likely because the molecular weight is low. However, there appears a downward shift in the thermal scan in the temperature range from 0 to 50 °C, the cause of which is unknown. For the blend curve, the glass transition of the PEG block cannot be detected at −68 °C but a glass transition appears around 78 °C. Since the T_g of the PMMA sample used in this study is determined to be around 100 °C, the glass transition at 78 °C is assigned to the compatible PMMA/PEG phase. Since the weight ratio of the PEG and the PMMA in the blend is estimated to be around 6/100, the lowering of the PMMA T_g is not surprising. The morphology of the 40/60 blend was observed under POM, and the micrograph is shown in Figure 5D. Amid the dark PMMA phase, slightly bright domains are randomly distributed. Unlike the morphology of the 5/95 blend, the copolymer in the 40/60 blend tends to be less aggregated. There are no liquid crystalline regions present, and it seems that the rigid rods are randomly oriented. Therefore, the block copolymer is dispersed to a greater degree in the PMMA matrix in the 40/60 blend than in the 5/95 blend. The increase of the PEG content vs PMMA in the blend from 0.4/100 to 6/100 improves dispersion.

This blend material (40/60) was then subjected to the DMA measurements using the tension-film mode. The first DMA experiment was performed at a frequency of 1.0 Hz to determine the temperature dependence of the (tensile) storage modulus and the loss modulus, which are shown in Figure 7parts A and B, respectively. For the PMMA film, the storage modulus is maintained at a high value of ∼1500 MPa from room temperature to about 100 °C before suddenly dropping at higher temperatures. Note that the T_g of PMMA is near 100 °C. The drop in storage modulus is accompanied by the loss modulus peak at the same temperature. In the PHIC-*b*-PEG/PMMA blend (40/60), the loss peak appears at ∼77 °C, the glass transition temperature of the blend.

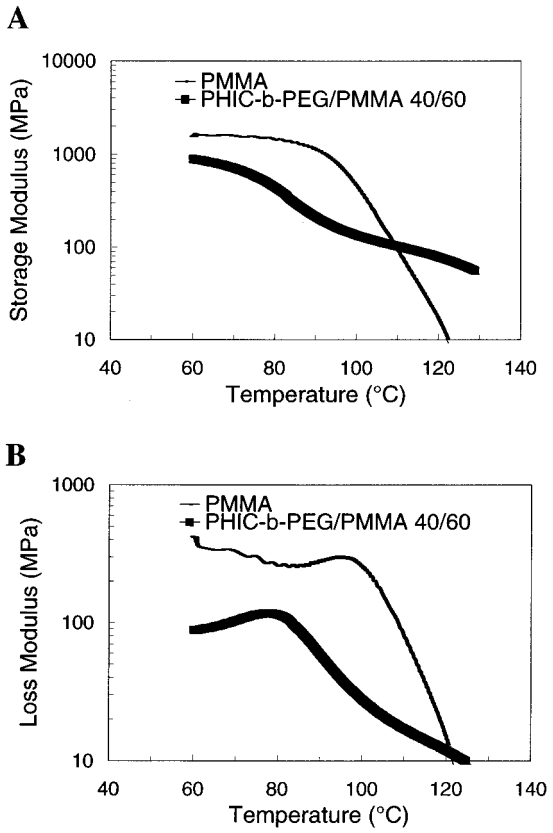

Figure 7. Temperature dependence of the (A) tensile storage modulus and (B) loss modulus of the PMMA and its blend with the PHIC-*b*-PEG block copolymer (60/40).

Again, we do not see any transition that can be assigned to the PHIC block. We notice that although the modulus of the blend is lower at room temperature than that of PMMA, it has a value of ~100 MPa at 120 °C whereas the modulus of PMMA is less than one-tenth of that value. This is a clear demonstration of the reinforcing effect of the rigid component at high temperatures.

The second DMA experiment we performed was the creep experiment at temperatures above the T_g of the blend (77 °C). Under a certain stress, the film underwent elongation and the strain gradually increased until at some point the material yielded. The purpose of the experiment was to see how the randomly oriented rods respond to tensile deformation. The results of the creep experiments are shown in Figure 8. The creep experiments were performed under a stress of 1.000 MPa at 80, 90, 95, and 100 °C. All four curves indicate increases in creep compliance as a function of time. At 80 °C, the creep compliance jumps immediately upon deformation, and then only increases gradually. The slope of the curve decreases very quickly at the beginning and levels off afterward. But there is no sign of yielding even after ~300 min. At 90 °C, the change in creep compliance has the same trend as that at 80 °C except the slope of the curve continues to increase after ~220 min and the film finally yields after ~250 min. Similar trends are seen at 95 and 100 °C. However, the increase of the slope occurs at ~40 and ~30 min, and yielding is observed at ~60 and ~45 min, respectively. The maximum change in strain during drawing is 30%. The appearance of the blend film changes from nearly transparent to completely opaque. We believe that the sudden jump of creep compliance at the beginning comes from the drawing of the matrix. Afterward, the gradual increase in creep compliance is caused by the gradual reorientation of the rigid rods along the drawing direction. This reorientation process proceeds much faster at higher temperatures and it ends when the increase of the slope occurs. At the last stage of the drawing, the material is further stretched and finally yields. The reorientation hypothesis is borne out not only by the opaque appear-

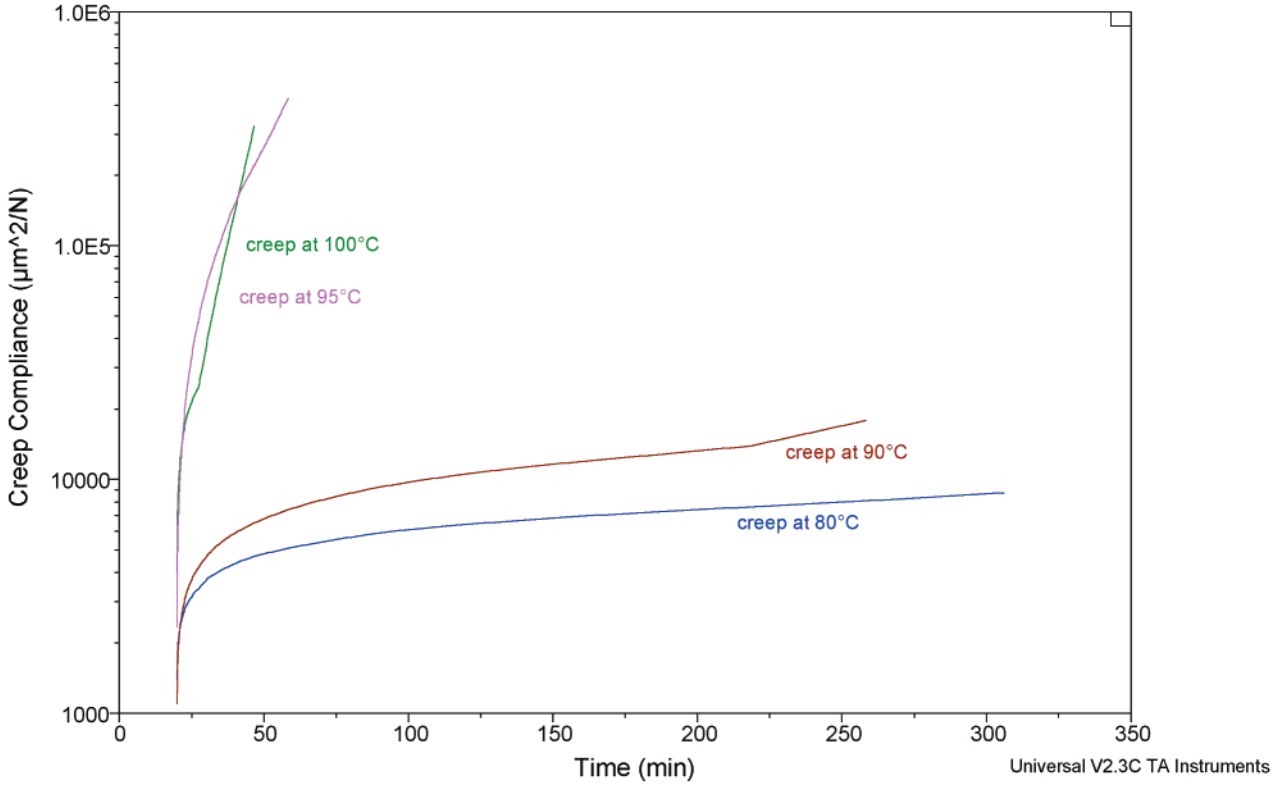

Figure 8. Time dependence of the creep compliance of the PHIC-*b*-PEG/PMMA blend (40/60) at various temperatures.

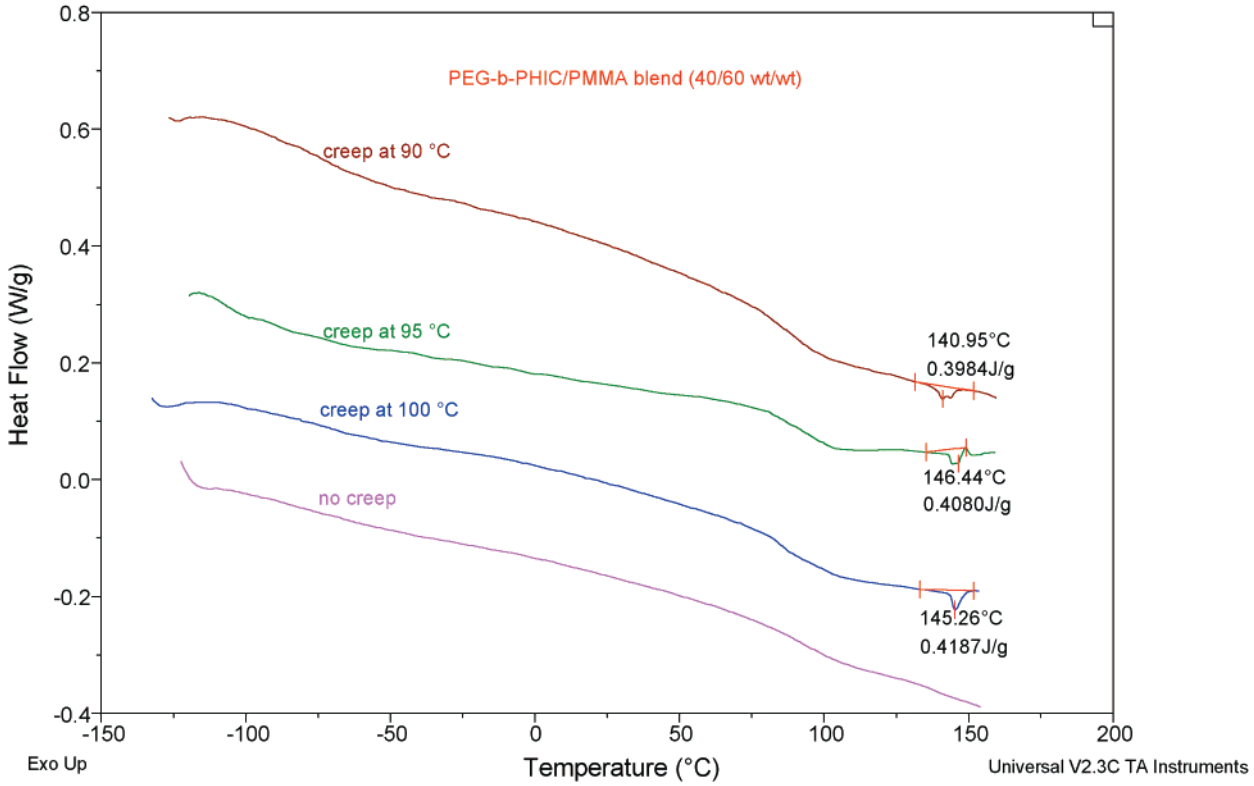

Figure 9. DSC thermograms of the PHIC-*b*-PEG/PMMA blend (40/60) samples after creep at various temperatures. (The untouched sample was used as comparison, and all the curves were extracted from the first heating run.)

ance of the film after drawing but also by the following DSC measurements of the drawn films.

DSC measurements were performed by thermally scanning the sample after a heating−cooling cycle. The thermograms of the PHIC-*b*-PEG/PMMA (40/60) blend samples after creep experiments at different temperatures are shown in Figure 9. The virgin blend sample was also tested for comparison. Compared to the virgin sample, there appears a small but sharp endothermic peak for each blend sample after creep. The endothermic event is located at around 140 °C, and the enthalpy associated with this transition is estimated as ∼0.4 J/g. If the samples are thermally scanned again, these peaks do not appear, and the transition is irreversible. We believe that the transition is related to the melting of the ordered clusters that formed from the reorientation of the rods during the creep process. The value of the associated enthalpy is comparable to that from the melting of liquid crystalline domains. This stretch-induced reorientation of the rigid-rod polymer might further improve the tensile strength of the material.

Conclusions

A novel rod−coil block copolymer poly(*n*-hexyl isocyanate)-*b*-poly(ethylene glycol) was synthesized using the titanium(IV)-catalyzed living coordination polymerization method. The PHIC-*b*-PEG rod−coil block copolymer exhibited lyotropic mesophases in concentrated toluene solutions. The solution became birefringent without any apparent orientation of the block copolymer when the concentration was above 20 wt %. Beyond 30 wt % of the block copolymer in toluene, the solution was still birefringent but with an apparent orientation direction of the block copolymer. The solution formed a transparent gel at the concentration of 45 wt %.

The morphology of the block copolymer in solid state consisted of nematic-like domain texture with ∼1 μm in size when the block copolymer film was cast from the 0.4 wt % toluene solution. The texture remained similar but the domain sizes became smaller when the film was cast from a chloroform solution, which was due to the slight conformation change of the helix in chloroform. The liquid-crystalline texture was completely erased when cast from a toluene/pentafluorophenol solution, where the PFP converted the rod configuration of the PHIC block into the coil configuration.

Polymer blends of the block copolymer with PMMA exhibited some compatibility. The compatibility was improved when the amount of the PEG block was increased in the blend. The 40/60 blend exhibited more compatible with PMMA than the 5/95 blend. The DMA measurements indicated better tensile strength property of the 40/60 blend at high temperatures above the T_g of PMMA itself. The 40/60 blend also showed ordered clusters of the rigid rods after the sample had undergone creep experiments, which might further improve the tensile strength of the material. In addition, the 5/95 PHIC-*b*-PEG/PMMA and PHIC-*b*-PEG/PVAc blends exhibited liquid crystalline domains in the solid state.

Acknowledgment. The authors wish to thank Professor Edith Turi for using the Professor Edith Turi Thermal Analysis Laboratory.

References and Notes

(1) (a) Jenekhe, S. A.; Chen, X. L. *Science* **1998**, *279*, 1903−1907. (b) Chen, J. T.; Thomas, E. L.; Ober, C. K.; Hwang, S. S. *Macromolecules* **1995**, *28*, 1688−1697. (c) Loos, K.; Stadler, R. *Macromolecules* **1997**, *30*, 7641−7643. (d) Kukula, H.; Ziener, U.; Schöps, M.; Godt, A. *Macromolecules* **1998**, *31*, 5160−5163. (e) Cornelissen, J. J. L. M.; Fischer, M.; Sommerdijk, N. A. J. M.; Nolte, R. J. M. *Science* **1998**, *280*, 1427−1430. (f) Radzilowski, L. H.; Stupp, S. I. *Macromolecules* **1994**, *27*, 7747. (g) Lee, M.; Oh, N. K.; Lee, H. K.; Zin, W. C. *Macromolecules* **1996**, *29*, 5567−5573.

(2) (a) Semenov, A. N.; Vasilenko, S. V. *Sov. Phys. JETP* **1986**, *63*, 70. (b) Semenov, A. N. *Mol. Cryst. Liq. Cryst.* **1991**, *209*, 191. (c) Halperin, A. *Macromolecules* **1990**, *23*, 2724. (d) Halperin, A. *Europhys. Lett.* **1989**, *10*, 549. (e) Williams, D. R. M.; Fredrickson, G. H. *Macromolecules* **1992**, *25*, 3561. (f) Raphael, E.; de Gennes, P. G. *Makromol. Chem. Macromol. Symp.* **1992**, *62*, 1.
(3) Takayanagi, M. *Trends Appl. Chem.* **1983**, *55*, 819−832.
(4) Hwang, W.-F.; Wiff, D. R.; Verschoore, C.; Price, G. E. *Polym. Eng. Sci.* **1983**, *23*, 784−788.
(5) (a) Petekidis, G.; Vlassopoulos, D.; Fytas, G.; Fleischer, G. *Macromolecules* **1998**, *31*, 1406. (b) Schmidt, A.; Lehmann, S.; Georgelin, M.; Katana, G.; Mathauer, K.; Kremer, F.; Schmidt-Rohr, K.; Boeffel, C.; Wegner, G.; Knoll, W. *Macromolecules* **1995**, *28*, 5487. (c) Drogemeier, J.; Eimer, W. *Macromolecules* **1994**, *27*, 96. (d) Keep, G. T.; Pecora, R. *Macromolecules* **1984**, *18*, 1167; **1988**, *21*, 817.
(6) Ji, S. H.; Zin, W. C.; Oh, N. K.; Lee, M. *Polymer* **1997**, *38*, 4377−4380.
(7) Clough, S. B. In *Characterization of Materials in Research Ceramics and Polymers*; Burke, J. J., Weiss, V., Eds.; Syracuse University Press: Syracuse, NY, 1975; pp 417−436.
(8) Berger, M. N. *J. Macromol. Sci.—Rev. Macromol, Chem.* **1973**, *C9* (2), 269.
(9) (a) Bur, A. J.; Fetters, L. J. *Chem. Rev.* **1976**, *76*, 6, 727. (b) Fetters, L. J.; Yu, H. *Macromolecules* **1971**, *4*, 385.
(10) (a) Martuscelli, E.; Pracella, M.; Yue, W. P. *Polymer* **1984**, *25*, 1097−1106. (b) Martuscelli, E.; Demma, G. B.; Rossi, E.; Segre, A. L. *Polymer* **1983**, *24*, 266. (c) Rao, G. R.; Castiglioni, C.; Gussoni, M.; Martuscelli, E.; Zerbi, G. *Polymer* **1985**, *26*, 811.
(11) Martuscelli, E.; Silvestre, C.; Gismondi, G. *Makromol. Chem.* **1983**, *186*, 2161.
(12) Shih, H. Y.; Kuo, W. F.; Pearce, E. M.; Kwei, T. K. *J. Polym. Res. (Taiwan)* **1995**, *196*, 3107.
(13) Fetters, L. J. *Polym. Lett.* **1972**, *10*, 577−582.
(14) (a) Patten, T. E.; Novak, B. M. *J. Am. Chem. Soc.* **1991**, *113*, 5065. (b) Patten, T. E.; Novak, B. M. *Macromolecules* **1993**, *26*, 436.
(15) (a) Meth-Cohn, O.; Thorpe, D.; Twitchett, H. J. *J. Chem. Soc. C* **1970**, 132. (b) Chandra, G.; Jenkins, A. D.; Lappert, M. F.; Srivastava, R. C. *J. Chem. Soc. A* **1970**, 2550. (c) Clark, R. J. H.; Stockwell, J. A.; Wilkins, J. D. *J. Chem. Soc., Dalton Trans.* **1976**, 120.
(16) Jha, S. K. Dissertation, Polytechnic University, 1998.
(17) Wittmann, J. C.; Lotz, B.; Candau, F.; Kovacs, A. J. *J. Polym. Sci., Polym. Phys.* **1982**, *20*, 1341.
(18) Aharoni, S. M.; Walsh, E. K. *Macromolecules* **1979**, *12*, 271.
(19) Schreckenbach, A. *Polymer* **1997**, *38*, 3069.
(20) Elias, H. G. *Makromolekule*, 4th ed.; Huthig & Wepf: Basel, Switzerland, 1981; p 155.
(21) Basset, D. C. *CRC Crit. Rev. Solid State Mater. Sci.* **1984**, *12*, 97.

MA0011486